History of Medicine, 2023, 9(1): 2501–2508
DOI: 10.17720/2409-5834.v9.1.2023.324

Docking, ADMET Study, Synthesis and Biological Evaluation of Isoxazole Derivatives as Potential Histone Deacetylase Inhibitors

Ali Mohammed Saeed Abdulameer[1*], Ayad Abed Ali Al-Hamashi[2]

[1]*BSc. in Pharmacy, Ministry of health, Babel Healthcare Directorate, Inspection Department/Iraq*
Email: Ali.mohammed1200e@copharm.uobaghdad.edu.iq
[2]*Ph.D. in Pharmaceutical Chemistry / Department of Pharmaceutical Chemistry, College of Pharmacy, University of Baghdad/Iraq*
Email: a.alhamashi@copharm.uobaghdad.edu.iq

***Correspondence author:** Ali Mohammed Saeed Abdulameer (Ali.mohammed1200e@copharm.uobaghdad.edu.iq)

Received: 22 January 2023 **Accepted:** 15 April 2023

Citation: Abdulameer AMS, Al-Hamashi AAA (2023) Docking, ADMET Study, Synthesis and Biological Evaluation of Isoxazole Derivatives as Potential Histone Deacetylase Inhibitors. History of Medicine 9(1): 2501–2508. https://doi.org/10.17720/2409-5834.v9.1.2023.324

Abstract

As an epigenetic target, histone acetylation has great therapeutic value. Several disorders, including cancer, are associated with an increase in the activity of histone deacetylase enzymes (HDACs). The hydroxamate group is employed in most HDAC inhibitors, since it is a strong zinc binding molecule (ZBG). Due to their toxicity and poor pharmacokinetic, hydroxamates are not a preferred cancer therapy option. As a result, a possible technique for increasing potency and selectivity is the development of non-hydroximate HDAC inhibitors. By using Glide's Ligand Designer, we were able to create new HDAC inhibitors that had isoxazole moiety as ZBG. Many different aliphatic and aromatic residues were tried to find the best fit for the cap group and the linker. Using authorized Schrodinger modelling software, the potential inhibition over HDAC8 for the best designed items was synthesized and tested. The data demonstrated the effect of different connecting group with isoxazole as zinc binding group. To estimate the pharmacokinetic parameters of the final products, an ADMET/tox study was conducted. the resulting compounds have promising drug-like attributes. Both the intermediate and final chemicals were produced using mild condition procedures and purified using column chromatography. IR and NMR spectroscopy were used to characterize the chemical structure of the intermediates and the final products. The MTT assay was used to evaluate the inhibition activity against colon cancer cell line (ST-174), which indicated that there is a comparable antiproliferative activity to vorinostat for some of the synthesized compounds.

Keywords

Histone, Anti-cancer, HDAC8, Vorinostat, Molecular Modelling.

Cancer, Huntington's, Alzheimer's, Parkinson's illnesses, spinocerebellar ataxia, and amyotrophic lateral sclerosis are human disorders linked to abnormal epigenetic alterations. As one of the main fatalities, cancer has piqued the curiosity of many researchers to create a medicine that might halt the tumours (1). Abnormal epigenetic changes were shown to have a high association with cancer (2). Histone acetylation is a known epigenetic modification in the development of cancers and other diseases. The enzymes histone acetylase (HAT) and

histone deacetylase (HDAC) regulate the dynamic process of histone acetylation (1,3,4). Inhibiting the enzyme HDAC is an exciting direction in cancer treatment (5). HDAC, inhibitors of vorinostat, romidepsin, panobinostat, and belinostat are FDA approved for treating cancer as monotherapy or in combination with other anti-cancer medications. The hydroxamate moiety is ZBG in three of the clinically used HDAC inhibitors. Studies have shown that hydroxamate has a low therapeutic index and a significant potential for adverse effects. (6,7).

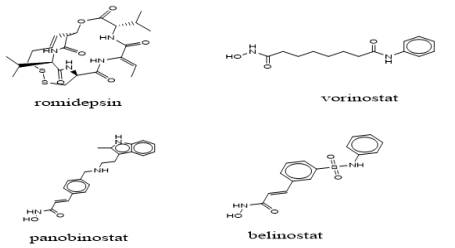

Figure 1. FDA approved HDAC inhibitors.(8)

In this work, Glide software was utilized (9), to conduct a docking investigation. FDA approved drug vorinostat was used in the design as reference. Ligand Designer for the creation of a new zinc binding group (ZBG), with a concentration on a heterocyclic ring. Isoxazole was suggested as a possible novel ZBG. A cap group and linker were-applied using the common pharmacophoric characters of HDAC inhibitors. An ADMET analysis was performed to foresee the pharmacokinetic properties of the suggested compounds in an effort to counteract the poor pharmacokinetics and toxicity of hydroxamate ZBG. A docking study of the designed compounds performed against HDAC8 (1T69) isoform downloaded from PDB (10), protein prepared using protein preparation wizard within the software, developed compounds created using ligand designer, then docked against prepared HDAC8 isoform (1T69) using highly precise XP docking strategy (9,11). Designed compounds with an acceptable docking score and fitness to the receptor were synthesized under moderate organic synthesis conditions. A preliminary antiproliferative activity was conducted to evaluate the cytotoxicity of the synthesized products.

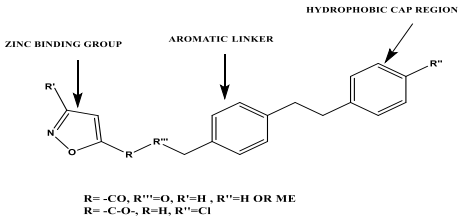

Figure 2. general pharmacophoric character of designed compound

Materials and Method

Molecular Docking

Docking study was performed using Glide application embeded with the maestro software from licensed Schrodinger's modelling suite version 13.0135. Vorinostat being utilized as a model structure. Ligand Designer suggest virtual compounds to design a novel zinc binding group. The molecules were finalized by inserting a cap group and a linker based on the general pharmacophoric features of reference compounds (9,12). HDAC8 (1T69) crystal structure was retrieved from the Protein Data Bank (www.rcsb.org) (13).

We used the protein preparation wizard to enhance the H-bond assignments, substitute hydrogen, add terminal oxygen to the chain, and remove water from the active site beyond position $3A^{0}$, and create a ligand with EpiK. Finally, we used the OPLS (2005) force field to clean up the structure. Grid was constructed for the co-crystallized ligand using the default settings, with the grid size limited to$15A^{o}$*$15A^{o}$*$15A^{o}$ (12,14). Virtual compounds obtained are prepared using ligaprep for the next step (9). The compounds for Ligprep nominated for docking against HDAC8 (1T69) using the default setting of XP docking limiting out to 10 pose. The generated poses were visualized by observing the fitness of the ligand into the active site with comparing docking score, XP H-bond, and e-model energy.

ADME-TOX Studies

To evaluate the drug-likeness of proposed compounds, prepared ligands with accepted docking score and fitness to

the protein undergo ligand ADME/tox prediction using QIKProp software adjust to find the five most relevant drug molecules, and the resulting data is tested for drug-ability of the created compounds in silico.(15)

Chemical Synthesis

Materials

Commercial sources provided the starting ingredients, reagents, and catalysts (Sigma Aldrich, Glentham, Fluorochem, Macklin, Liyan, Thomas Beaker, Merck). Molecular sieves 3A were utilized to dry all solvents used. TLC was performed using Merck KGaA TLC silica gel 60 254 sheet of 20*20 cm, spot applications performed under UV-light-lamp of 254 nm, detection performed under UV lamp or iodine vapour. Shimadzu IR-Affinity-1 Spectrometer (Shimadzu, Japan) was used for FT-IR spectroscopy at the University of Baghdad-College of Pharmacy. The ^{1}H-NMR and ^{13}C-NMR studies were performed using a Bruker Avance III, 400 MHz spectrometer at the University of Basra- College of Education, Department of Chemistry with 400 MHz and 100 MHz, respectively (d6 - DMSO as the solvent),.(16)

General procedure for the synthesis of 4-(((tert-butyldimethylsilyl)oxy)methyl)aniline (compound I)

To a mortar of 100 ml volume charged with 1.65 g of TBDMSCl (11 mmol), 1.23 gm of 4-aminobenzyl alcohol (10 mmol), 25 mmol imidazole, grinding using a pistol continue up to 4 minutes, monitored with TLC (ethylacetate:hexane) for the consumption of alcohol. The reaction quenched by adding hexane, filtered through filter paper, and solvent was removed. The yield is 95% of the product as pale-yellow coloured liquid. The product was used in the next reaction without further purification. I.R: 3363, 2954, 2927 ,2854, 1253 cm^{-1}. (17)

General procedure for the synthesis of compound II

To a round bottom flask equipped with a magnetic bar added **Compound I** (711 mg, 3 mmol), substituted or unsubstituted benzoic acid (3 mmol), EDC.HCl (573 mg, 3 mmol), HOBt (40 mg, 0.3 mmol), of DMAP (366 mg, 3 mmol), of DIPEA (775 mg, 6 mmol), and DCM (12 ml). TLC (1 ethyl acetate: 3 hexane) was used to follow the reaction progress which is completed at 12-18 hours depending on the carboxylic acid used. The resultant residue was washed with 10% $NAHCO_3$ and 5% HCl. Further purification was performed using column chromatography on neutralized silica gel using (ethyl acetate: hexane) as eluent to afford the products as white powder (18). Yield 75-90%.

N-(4-(((tert- butyldimethylsilyl) oxy)methyl) phenyl)-4-methylbenzamide (Compound IIa) yield is (80%). I.R: 3363, 3055, 2951, 2931, 2897, 2854, 1658, 1597, 1523 cm^{-1}. ^{1}H NMR (400 MHz, DMSO) δ 10.09 (s, 1H), 7.83 – 7.75 (m, 2H), 7.69 – 7.62 (m, 2H), 7.26 (d, J = 7.9 Hz, 2H), 7.23 – 7.16 (m, 2H), 4.59 (s, 2H), 2.31 (s, 2H), 0.82 (s, 8H).

N-(4-(((tert-butyldimethylsilyl)oxy)methyl)phenyl)benzamide (Compound IIb) IR: 3360, 2951, 2931, 1654, 1597, 1253, 1180, 1053 cm^{-1}. ^{1}H NMR (400 MHz, DMSO) δ 10.18 (s, 1H), 7.91 – 7.84 (m, 2H), 7.70 – 7.63 (m, 2H), 7.56 – 7.41 (m, 3H), 7.21 (d, J = 8.2 Hz, 2H), 4.60 (s, 2H), 0.82 (d, J = 5.7 Hz, 1H), 0.82 (s, 9H).

N-(4-(((tert- butyldimethylsilyl) oxy) methyl) phenyl)-4-chlorobenzamide (Compound IIc) IR 3360, 2951, 2931, 2858, 1654, 1597, 1523, 1253, 1063 cm^{-1}.

General procedure for the synthesis of compound III

To a 20 ml beaker, 1 mmol of **compound II** and 3 ml of dry methanol were added. At 0 C^{o}, 0.25 mmol of acetyl chloride (20 mg) was added, the reaction mixture is monitored by TLC (4 ethyl acetate in 10 hexane) for consumption of the starting material after 15-60 minutes. The solvent was evaporated, and the residue was quenched and neutralized by adding saturated sodium bicarbonate, solvent was removed. Silica column chromatography was performed using gradient eluent (hexane: ethyl acetate). Yield from this method is 70-80% as white powder.(19)

N-(4-(hydroxymethyl)phenyl)-4-methylbenzamide (Compound IIIa) IR: 3336, 3052, 2916, 2864, 1651, 1597, 128 cm^{-1}. ^{1}H NMR (400 MHz, DMSO) δ 10.07 (s, 1H), 7.83 – 7.77 (m, 2H), 7.68 –

7.61 (m, 2H), 7.23 (dd, J = 18.5, 8.1 Hz, 4H), 5.08 (d, J = 4.7 Hz, 1H), 4.42 – 4.36 (m, 2H), 2.31 (s, 3H).

N-(4-(hydroxymethyl)phenyl)benzamide (Compound IIIb) IR: 3344, 3053, 2924, 2864, 1651, 1600, 1523 cm^{-1}. ^{1}H NMR (400 MHz, DMSO) δ 10.26 (s, 1H), 7.98 (d, J = 7.5 Hz, 2H), 7.76 (d, J = 8.1 Hz, 2H), 7.63 – 7.55 (m, 1H), 7.53 (t, J = 7.4 Hz, 2H), 7.32 (d, J = 8.2 Hz, 2H), 5.19 (t, J = 5.7 Hz, 1H), 4.49 (d, J = 5.7 Hz, 2H).

4-chloro-N-(4-(hydroxymethyl)phenyl) benzamide (Compound IIIc) IR: 3321, 3051, 2935, 2861, 1641, 1597, 1521, 1002 cm^{-1}.

General procedure for the synthesis of compound VI

A solution of iodine (1.5 mmol) in 20 ml of dried dichloromethane is prepared in 50 ml flask emersed with crushed ice bath to lower the temperature to 0 C^0, triphenylphosphine (1.5 mmol) was added to produce a brown solution; imidazole (3 mmol) is added to produce a yellow solution. Carboxylic acid was added, the resulting mixture is swirled 0 C^0 for 15-20 minutes before adding compound III, swirling continued for 4 hour (monitored by TLC for completion of the consumption of the starting material), reaction mixture stirred overnight to ensure completion of the reaction, filtered through sodium thiosulfate; if sticky triturate with hexane; to give a pale brown-colored crude product which purified by column chromatography (ethyl acetate : hexane) to give a white color thread like powder. Yield is 35-60% as white needle shape crystals. (20)

Compound VIa IR: 3383, 3143, 2920, 2850, 1724, 1651, 1597, 1280, 1233, 1130 cm^{-1}. $^{1}HNMR$(400 MHz, DMSO) δ 10.28 (s, 1H), 8.87 (d, J = 1.9 Hz, 1H), 7.89 (d, J = 8.0 Hz, 2H), 7.86 – 7.80 (m, 2H), 7.50 – 7.44 (m, 2H), 7.35 (dd, J = 5.0, 3.1 Hz, 3H), 5.37 (s, 2H), 2.39 (s, 3H). ^{13}C NMR (101 MHz, DMSO) δ 165.89, 159.38, 156.63, 152.61, 142.16, 140.04, 132.37, 130.35, 129.68, 129.40, 128.20, 128.13, 127.24, 120.72, 120.57, 110.24, 67.61, 21.50.

Compound VIb IR :3356, 3097,2920, 1728, 1651, 1284, 1207, 1141 cm^{-1}. ^{1}H NMR (400 MHz, DMSO) δ 10.37 (s, 1H), 8.89 – 8.84 (d, 1H), 8.00 – 7.93 (d, 2H), 7.84 (d, J = 8.4 Hz, 2H), 7.65 – 7.45 (m, 5H), 7.34 (d J = 1.4 Hz, 1H), 5.37 (s, 2H). ^{13}C NMR (101 MHz, DMSO) δ 166.11, 159.38, 156.63, 152.61, 139.96, 135.28, 132.14, 130.48, 129.69, 128.88, 128.16, 120.74, 110.24, 67.60.

Synthesis of compound V

To a Schlenk flask of 25 ml, 1 mmol of **compound III** and 4 ml acetonitrile were added under argon, stirred at room temperature for 2 hour , monitored with TLC, then 3-methyl, 5 bromomethyl isoxazole was added (1.5 mmol) with continuous stirring under argon for the next 18 hour. After completion of the reaction monitored by TLC, the mixture was filtered to remove cesium carbonate. Solvent removed to give a sticky mass which purified using column chromatography (ethyl acetate : hexane) to produce a white wool like powder, yield 30-40% (21). I.R; 3367, 3128,2962, 2852, 1712, 1654, 1597, 1527, 1263, 1172, 1091 cm^{-1}, ^{1}H-NMR (400 MHz, DMSO) δ 10.41 (s, 1H), 8.05 – 7.96 (m, 4H), 7.86 – 7.79 (m, 2H), 7.67 – 7.58 (m, 4H), 7.52 – 7.46 (m, 2H), 6.42 (s, 1H), 5.34 (s, 2H), 4.66 (s, 2H), 2.24 (s, 3H). ^{13}C-NMR (101 MHz, DMSO) δ 168.36, 165.26, 164.94, 160.00, 139.48, 138.84, 136.94, 133.98, 131.62, 131.57, 130.13, 129.48, 129.29, 128.95, 120.84, 105.13, 66.78, 62.84, 11.40.

Cell line study

The goal of the MTT testing is to assess cell survival with no need for sophisticated cell counting. Consequently, the most common use is to investigate the cytotoxicity. The MTT test identifies the mitochondrial activity of viable cells, and a linear relationship exists between the quantity of viable cells and mitochondrial activity. The transformation of the yellow tetrazolium salt (MTT dye) into dark purple formazan crystals by NADH, which may involve for homogenous calculations give an idea about the mitochondrial inactivity of the cells, is indicative of the mitochondrial activity of the cells. Thus, any increase or decrease in viable cell culture may be observed by measuring the absorbance using a plate reader at 570 nm and monitoring formazan-concentration. The darker the mixture, the greater the number of living and metabolically active cells present (22).

Vorinostat, compound **V**, and compound **VIa** are chosen for cell line assay with colon cancer cell type St174, the stock for all is choose is 100 mg/1ml, with serial dilution at 50% for each 50 mg/ml , 25 mg/ml , 12.5 mg/ml , 6.25 mg/ml and 31.125 mg/ml. 2 'l of the above dilutions was added to 198 'l of cell line and incubate for 24 hours. The final concentration is 1 'l of different dilutions mentioned above in 1'l of cell line. After the drug exposure period was complete, the medium was removed from the wells and the cells washed with PBS. To assess formazan residue, a blank control was used. After that, each well was filled with 198 µl of the resulting solution. Plate was incubated at 37°C for 3 hours until purple intracellular formazan crystals were visible under an inverted microscope. After the supernatant was removed, 100 µl of DMSO was added to each well to dissolve the resultant formazan crystals. The plate was incubated for 30 minutes at room temperature until the cells lysed and the purple crystals dissolved.

The percentage of cell viability or proliferation was calculated by dividing the absorbance readings of test samples by those of the control samples and multiplying by 100. Absorbance levels larger than the control indicate cell growth, while absorbance values less than the control indicate cell death or suppression of cell proliferation. The proportion of cell viability or inhibition was computed using the following formula.

$$\% \text{ viability} = (AT - AB) / (AC - AB) \times 100\%$$

Where, AT = Absorbance of treated cells (drug).
Absorbance of blank (only medium).
AC = Absorbance of control (untreated).
% Inhibition = 100 – % viability

Results and Discussion

Docking Study

The docking scores for compounds **VIa** and **VIb** and **V** on HDAC8 were -5 to -8 kcal/mole as well as accepted fitness to the receptor. The bonds that involved interacting with the active site of the receptor for the proposed compounds are visualized including H-bond, π-π staking, and interaction with zinc ion within the active site. Docking score indicate energy involved when ligand interact with the active site, considering flexible ligand docking. Visual assessment of the fitness and the type of bond involved, emodel, Glide score, EpiK and Glide energy. These factors with visual inspections, can predict virtual fitness to ± the active site, even when docking score are high, the compound may not interact with the active site. Compound **V** show binding to the zinc ion in bidentate interaction while the rest compounds show monodentate interaction with zinc ion, although docking score show better fitness of compound **VIa** and **VIb** (Figures 3 and Table 1) (9,14).

Table 1. Docking parameters of final compounds on HDAC8.

	Compound	Docking score (kcal/mole)	e-model	Xp energy	e-inernal	Xp H-bond
1.	Vorinostat	-9.071	-67.433	-41.728	9.285	-1.462
2.	VIa	-8.403	-41.365	-41.365	2.849	-0.865
3.	VIb	-7.575	-73.202	-40.971	3.762	-0.964
4.	V	-5.201	-67.433	-43.317	6.703	0.461

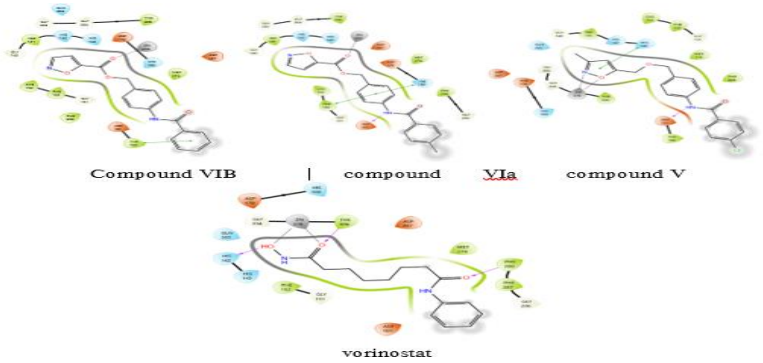

Figure 3. 2D interaction diagram of the final compounds and vorinostat with HDAC8 (1T69).

The relationship between Emodel and Glide energy is quite complex (unlike Glide Gscore). Emodel is used to determine the optimal posture among all conformations obtained after docking. Once the pose is identified, only the docking score (Glide Gscore + Epik) for this molecule is used for reporting binding affinity. Emodel is a combination of Glide Gscore, Glide energy, and ligand strain energy. Without scaling, the glide energy represents the coulomb and vdw interactions between the protein and the ligand.

The internal energy ('Einternal') is the extra internal energy of a posture compared to the pose with the lowest energy and is calculated using simplified version of the OPLS 2005 force field that only contains torsions and 1,4 vdW interactions. The compound **VIa** shows a comparable docking score to vorinostat, while the compound **V** have the lowest docking score (Table 1). As well as the visual inspection indicated that compound **V** shows a virtual monodentate interaction with zinc ion inside the active site.

ADME-TOX Studies

Many structural features and properties should be considered for the designed molecules to act as drug-like molecule. The virtual estimation of rule of five for structural features and rule of three for orally administered drug are evaluated to avoiding expensive late preclinical trial and clinical trials frustration. Orally bioavailable drug-like chemical definition in respect to estimated molecular descriptors has greatly aided synthetic medicinal chemists' efforts. Lipinski was the first to introduce, and then additional augmentation by Veber and co-workers which stated that their guidelines not only impact decision for synthetic reasons, but it is also it is crucial in the selection of compounds for screening libraries received from commercial suppliers. Compounds (**V** and **VI**) have an accepted pharmacokinetic property. (23–25)

Table 2. ADME/tox of the proposed compound and vorinostat.

Title	#stars	#rotor	#rtvFG	CNS	#metab	PercentHuman OralAbsorption	RuleOfFive	RuleOfThree
Vorinostat	0	9	1	-2	3	67.516	0	0
V	0	6	0	-1	4	100	0	1
VIb	0	5	0	-2	1	86.86	0	0
VIa	0	5	0	-2	2	88.338	0	0

From the table 2, its predicted that final compounds have no violation to the rule of five or rule of three, which make them assigned as drug-like molecules. Furthermore, the rotational functional group (rtvFG) which is the number of functional group that undergo metabolism to unwanted or toxic group, is absent in the

synthesized compound. Vorinostat as previously known it metabolized to toxic by-product hydroxylamine or metabolized in plasma to corresponding carboxylic acid leading to decrease activity (26), the proposed compounds above lack this toxicity as listed in the table 2. In conclusion, the final compounds showed higher estimated metabolism stability and better oral bioavailability, combining docking score with ADMET study, compound **VIa** show an accepted drug like character.

Chemical Synthesis

The synthesis of the proposed compound begins with 4-aminobenzylalcohol protection to direct the reaction toward the amine to form amide, this is achieved by mild condition with the use of TBDMSCl as protecting agent and imidazole as catalyst. This reaction was performed using solvent free grinding method as green method avoiding the use of environmental toxic solvent to offer simple rapid, high yield and simple workup procedure reaction. The appearance of amide IR absorption peak near 3350 with the disappearance of O-H stretching peak at 3256 cm^{-1} indicating the formation of compound **I** (27). Compound **II** prepared from compound **I** using HOBt, EDC, DMAP, and DIPEA to form amide bond (28). Compound **III** was synthesized by the deprotection compound **II** using acetyl chloride in dry methanol. Compound **VI** was produced by Michalis addition of compound **III** and isoxazole 5-carboxylic acid using triphenylphosphine, imidazole (20). Compound **V** was synthesized through the reaction of 3-methyl,5-bromomethyl isoxazole with compound **III** to form ether using modified Williamson ether synthesis method(29). Final compounds and intermediates were purified using column chromatography and characterized by FTIR and NMR.

Field Code Changed

Cell Line Study

The colon cancer cell line (st174) was used for this work. The MTT assay after incubation for 24 hours shows a promising inhibition activity that is comparable to vorinostat. More specifically, compound **VIa** compared has a single digit micromolar inhibition activity that comparable to vorinostat. While compound **V** that involve ether bond to connect isoxazole to linker moiety showed no cancer cell inhibition even at 28""""

Table 3. IC50 for the final compounds and vorinostat.

Compound	Structure	IC50
VIa	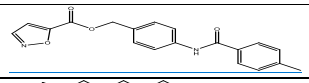	"""""""
V	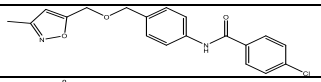	No activity at 28""""
Vorinostat	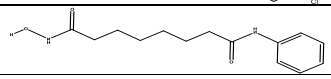	0.62 "'

Conclusion

Potential HDAC inhibitors were designed by instillation of new zinc binding group of isoxazole. The zinc chelation tendency was virtually studied through the molecular docking studies using the licensed Glide software. Final compounds showed accepted pharmacokinetic properties through the virtual ADMET studies. The designed compounds were successfully synthesized applying the excellent mild organic synthesis methods with accepted yields. The intermediates and final products were characterized by FTIR and NMR spectroscopy. The biological studies for the synthesized compounds indicated that the ether containing compound **VIa** showed a sub-micromolar IC_{50} which is comparable to vorinostat, while compound **V** that involve ether moiety connecting the ZBG to linker showed no activity. These findings are compatible with the molecular docking results. The enzymatic inhibition studies for final compounds will be performed to confirm the theoretical inhibition activity HDAC isoforms.

References

Cheng Y, He C, Wang M, Ma X, Mo F, Yang S, et al. Targeting epigenetic regulators for cancer therapy: mechanisms and advances in clinical trials. Signal Transduct Target Ther. 2019 Oct 24;4(1):62.

Jenke R, Reßing N, Hansen FK, Aigner A, Büch T. Anticancer Therapy with HDAC Inhibitors: Mechanism-Based Combination Strategies and Future Perspectives. MDPI [Internet]. 2020 Dec 30;13(4):634. Available from: https://doi.org/10.3390/cancers13040634

Lu Y, Chan YT, Tan HY, Li S, Wang N, Feng Y. Epigenetic regulation in human cancer: the potential role of epi-drug in cancer therapy. Mol Cancer. 2020 Apr 27;19(1):79.

Alwash AH, Alani BG, Ibrahim IT. RECENT PROGRESS IN DEVELOPING SELECTIVE HISTONE. kerbala.jps. 2021 Apr 24;Pages 28-50.

Al-Amily D, Mohammed MH. Design, Synthesis and Cytotoxicity Study of Primary Amides as Histone Deacetylase Inhibitors. Iraqi J Pharm Sci. 2019;Vol.28(2) 2019:151–8.

Al-Hamashi AAAC. Design, Synthesis, and Biological Evaluation of Novel Histone Deacetylase Inhibitors as Anti-Cancer Agents. 2018.

Al-Hamashi AA, Abdulhadi SL, Ali RMH. AfterCarfulRevisiontemplateofEgyptian_AH_08282022.pdf. Egyptian Journal of Chemistry [Internet]. 2022 Aug 27; Available from: http://ejchem.journals.ekb.eg/

Vema A, Debnath S, Kalle AM. Identification of novel HDAC8 selective inhibitors through ligand and structure based studies: Exploiting the acetate release channel differences among class I isoforms. Arab J Chem. 2022;15(6):103863.

Friesner, Murphy RA;, Repasky RB;, Frye MP;, Greenwood LL;, Halgren JR;, et al. "Extra Precision Glide: Docking and Scoring Incorporating a Model of Hydrophobic Enclosure for Protein-Ligand Complexes," 2006, 49, 6177–6196. J Med Chem,. 2006;49, 6177–6196(49, 6177–6196).

RCSB PDB - 1T69: Crystal Structure of human HDAC8 complexed with SAHA [Internet]. [cited 2022 May 13]. Available from: https://www.rcsb.org/structure/1T69

Jorgensen WL, Tirado-Rives J. The OPLS [optimized potentials for liquid simulations] potential functions for proteins, energy minimizations for crystals of cyclic peptides and crambin. J Am Chem Soc. 1988;110(6):1657–66.

Halgren TA, Murphy RB, Friesner RA, Beard HS, Frye LL, Pollard WT, et al. Glide: a new approach for rapid, accurate docking and scoring. 2. Enrichment factors in database screening. J Med Chem. 2004;47(7):1750–9.

Somoza JR, Skene RJ, Katz BA, Mol C, Ho JD, Jennings AJ, et al. Structural Snapshots of Human HDAC8 Provide Insights into the Class I Histone Deacetylases. Structure. 2004;12(7):1325–34.

Sastry GM, Adzhigirey M, Day T, Annabhimoju R, Sherman W. Protein and ligand preparation: parameters, protocols, and influence on virtual screening enrichments. J Comput Aid Mol Des. 2013;27(3):221–34.

Arabia D of C and PET Jubail Industrial College (JIC), PO Box 10099, Jubail Industrial City 31961, Kingdom of Saudi, Alsawalha M, Bolla SR, Kandakatla N, Srinivasadesikan V, Veeraraghavan VP, et al. Molecular docking and ADMET analysis of hydroxamic acids as HDAC2 inhibitors. Bioinformation. 2019;15(6):380–7.

Judd CS, Morrisett JD, Chari MV, Browning JL. Proton NMR Basics. J Chem Educ. 1995;72(8):706.

Bartoszewicz A, Kalek M, Nilsson J, Hiresova R, Stawinski J. A New Reagent System for Efficient Silylation of Alcohols: Silyl Chloride-N -Methylimidazole-Iodine. Synlett. 2008;2008(1):37–40.

Ghoshſt AK, Shahabi D. synthesis of amide derivative for electron deficient amines and functionalized carboxylic acid using EDC and DMAP and a catalyst amout of hobt as coupling reagent.pdf. elesver. 2019;

Khan AT, Mondal E. A Highly Efficient and Useful Synthetic Protocol for the Cleavage of tert-Butyldimethylsilyl (TBS) Ethers Using a Catalytic Amount of Acetyl Chloride in Dry Methanol. Cheminform. 2003;34(31).

Morcillo SP, Cienfuegos LA de, Mota AJ, Justicia J, Robles R. Mild Method for the Selective Esterification of Carboxylic Acids Based on the Garegg–Samuelsson Reaction. J Org Chem. 2011;76(7):2277–81.

Xu ZY, Xu DQ, Liu BY. WILLIAMSON REACTION IN IONIC LIQUIDS. Org Prep Proced Int. 2004;36(2):156–61.

Meleady P, O'Connor R. Cell Biology (Third Edition). Part Cell Tissue Cult Assoc Techiniques Sect 1general Techniques Sect 1 Gen Techniques. 2006;(Cancer Res.121952):13–20.

Jorgensen WL. The Many Roles of Computation in Drug Discovery. Science. 2004;303(5665):1813–8.

24. Kouassi1 KAR, Ganiyou2 A, Benié1 A, Koné1 MGR, Nobel1 N kouakou, Bohoussou1 KV, et al. Identification of Potential C-kit Protein Kinase Inhibitors Associated with Human Liver Cancer: Atom-based 3D-QSAR Modeling, Pharmacophores-based Virtual Screening and Molecular Docking Studies [Internet]. 2019 [cited 2022 Aug 22]. Available from: http://www.sciepub.com/reference/350880

25. Yadav R, Imran M, Dhamija P, Chaurasia DK, Handu S. Virtual screening, ADMET prediction and dynamics simulation of potential compounds targeting the main protease of SARS-CoV-2. J Biomol Struct Dyn. 2020;39(17):6617–32.

26. Flipo M, Charton J, Hocine A, Dassonneville S, Deprez B, Deprez-Poulain R. Hydroxamates: Relationships between Structure and Plasma Stability. J Med Chem. 2009;52(21):6790–802.

27. Mittersteiner M, Voigt MA, Jesus PC de, Brondani PB. Solvent and Catalyst-Free Synthesis of Silicon-Protected Alcohols. Chem. 2018;3(38):10717–20.

28. Ghosh AK, Shahabi D. Synthesis of amide derivatives for electron deficient amines and functionalized carboxylic acids using EDC and DMAP and a catalytic amount of HOBt as the coupling reagents. Tetrahedron Lett. 2020;63:152719.

29. Dueno EE, Chu F, Kim SI, Jung KW. Cesium promoted O-alkylation of alcohols for the efficient ether synthesis. Tetrahedron Lett. 1999;40(10):1843–6.